

## Computer simulation of radiation acceleration mode in laser-plasma interaction\*

D.N. Gorpichenko, G.I. Dudnikova

**Abstract.** We present numerical studies on the ion acceleration from thin foils irradiated by ultra-high contrast laser pulses. Two-dimensional particle-in-cell (PIC) simulations reveal that ions are for a certain time accelerated in a phase-stable way by the laser radiation pressure. The development of the Rayleigh–Taylor instability leads to destroy foils and to decelerate the ion acceleration rate.

### 1. Introduction

Currently, the development in the laser technologies have enabled a high-power laser to produce multi-terrawatt femtosecond pulses. Nowadays, the interaction of a high-intensity laser pulse with plasma is a subject of interest for fundamental physics and numerous practical applications [1, 2].

Recent works indicate to the fact that under proper conditions the interaction of ultra-short, high-power lasers with thin foils can generate ion beams within 100–200 MeV energy range with relatively a low velocity dispersion [3, 4]. This technology can have the major implications to the medical proton cancer therapy since it can provide a relatively inexpensive table-top alternative to the currently used standard cyclotrons [5].

The generation of high-energy ions by the laser-plasma interaction has become attractive since the pioneer work that was realized ten years ago [6–8]. In these papers, the target normal sheath acceleration (TNSA) mechanism guiding the action of the emission of multi-MeV ion beams was studied. In the TNSA, the energy electrons are generated at the plasma surface, and quasi-static electric fields of order TV/m are created. As results ions acceleration was occurred with cut-off energy up to 60 MeV.

Recently, a new mechanism, the RPA (radiation pressure acceleration), for ion acceleration was proposed [9–11]. In this mode, protons are accelerated together with an electron cloud. The radiation pressure accelerates an electron cloud, which in turn accelerates ions due to the induced longitudinal charge separation fields. In contrast to the TNSA mode, the RPA mechanism is highly efficient, and the ion energy is proportional to the electromagnetic energy of a laser pulse. The pulsed Laser Driven acceleration of plasma sheets in the 1D scenario demonstrate that the proton energy up to

---

\*Supported by the Russian Foundation for Basic Research under Grant 09-02-01103.

200 MeV could be attained while the beam remains largely a mono-energy one [12]. In realistic 2D/3D geometries, the development of the Rayleigh–Taylor (R-T) instability of a plasma sheet is an obstacle for sustaining a quasi-mono-energy mode of the ion acceleration [13]. In fluid dynamics, the Raleigh–Taylor instability is a well-known phenomenon that occurs when a lighter fluid is accelerated into a heavier one. This instability also often takes place in magnetized plasma, where a magnetic field plays the role of a light fluid. For example, the R-T instability is very important in the case of an inertial fusion, where a fuel pellet is compressed by a high-intensity laser pulse.

The importance of both nonlinear and kinetic effects and a high dimensionality of the laser-plasma interaction process requires the computer-aided simulation. The key role of computer simulations is played by analysis of such extreme phenomena that are out of reach of analytical developments.

In order to describe the RPA mechanism of the particle acceleration, we consider numerical modeling of the laser pulse-plasma interaction based on fully relativistic 2D particle-in-cell (PIC) kinetic model [14]. In this paper, we present the results of the ion acceleration with circularly polarized (CP) laser pulses in a simple slab geometry and R-T instability.

## 2. Formulation of the problem

Let us consider the following problem. A high-intensity laser pulse falls onto the foil that is simulated as a thin slab of plasma consisting of electrons and ions. As a result of the laser-plasma interaction high-energy charged particles are generated. As this process is collisionless, then a kinetic plasma model based on the Vlasov equations can be used for the numerical simulation.

The initial system of equations includes the Vlasov equations for electron and ion plasma components and the Maxwell equations:

$$\begin{aligned} \frac{\partial f_\alpha}{\partial t} + (\vec{v}, \vec{\nabla}) f_\alpha + q_\alpha \left( \vec{E} + \frac{1}{c} [\vec{v}, \vec{B}] \right) \frac{\partial f_\alpha}{\partial \vec{p}} &= 0, \\ \frac{\partial \vec{B}}{\partial t} &= -c \operatorname{rot} \vec{E}, & \frac{\partial \vec{D}}{\partial t} &= c \operatorname{rot} \vec{H} - 4\pi \vec{j}, \\ \operatorname{div} \vec{B} &= 0, & \operatorname{div} \vec{D} &= 4\pi \rho, \\ \vec{p} &= \gamma m \vec{v}, & \gamma &= (1 - v/c)^{-1/2}, \\ \rho &= \sum_\alpha q_\alpha \int f_\alpha(\vec{v}) d\vec{v}, & \vec{j} &= \sum_\alpha q_\alpha \int \vec{v} f_\alpha(\vec{v}) d\vec{v}. \end{aligned}$$

Here, the subscript  $\alpha$  is used for electron and ion plasma components;  $f$  is a distribution function, and other variables have a standard designation.

To simulate the laser pulse-plasma interaction, we have carried out a series of the 2D particle-in-cell simulations with the fully relativistic code UMKA2D3V [14].

A laser pulse can be characterized by intensity, shape, and duration. Plasma can be characterized by shape and density. The plasma density can be described by a dimensionless parameter of the the ratio of plasma density to the critical density  $n_{\text{cr}}$ . When the plasma density  $n$  is equal to the critical density, the frequency of the laser  $\omega_0$  is equal to the Langmuir frequency  $\omega_{\text{oe}} = \sqrt{4\pi n e^2 / m_e}$ , i.e.,  $\omega_0 / \omega_{\text{oe}} = \sqrt{n_{\text{cr}} / n} = 1$ . If  $\omega_0 / \omega_{\text{oe}} > 1$ , plasma is described as underdense and transparent for the laser radiation. Plasma with  $\omega_0 / \omega_{\text{oe}} < 1$  is called the overdense plasma and the laser radiation can penetrate into plasma only at a distance of the skin depth  $\delta = c / \omega_{\text{oe}}$ .

In the simulation, a laser pulse is normally incident, impinges to the left on the axis  $x$ , and has a wavelength  $l$  an amplitude  $a$ , and a uniform spatial profile in  $y$  direction. A temporal profile of a laser pulse rises for several cycles and then remains constant. Simulations were performed for a normalized amplitude of the laser vector potential,  $a = eE_0 / m_e c \omega_0$ , where  $E_0$  is a vacuum electric field amplitude, and  $\omega_0$  is the frequency of a laser pulse ( $l = 2\pi c / \omega_0$ ),  $c$  is the speed of light,  $e$  is the electron charge, and  $m_e$  is the electron mass. The target plasma simulates a thin solid dense plasma slab of thickness  $d$  (foil). The foil has an electron density  $n$ , which is  $n$  times higher than the critical density  $n_{\text{cr}}$ . For a high intensity of a laser pulse,  $a \gg 1$ , the foil can be transparent for the electromagnetic radiation if  $d < a\lambda n_{\text{cr}} / n$ . This should be taken into account when choosing the size of foil. The total simulation box has  $4\lambda \times 60\lambda$  size, and the foil is located at  $x = 2\lambda$ .

To reduce boundary effects, there was considered a significantly longer vacuum region behind the foil. The boundary conditions for particles and electromagnetic fields are periodic in  $y$ -direction. In  $x$ -direction, the boundary conditions consist of the electromagnetic wave that enters the region at  $x > 0$  and freely leaves the computational domain at the right boundary. Particles are reflected from the boundaries in  $x$  direction. The initial particle velocity is equal to zero ( $\vec{v}_\alpha = 0$ ). We use the Cartesian mesh system with a uniform mesh size. The mesh width in  $x$  and  $y$  directions,  $\Delta_x$  and  $\Delta_y$ , respectively, are set to be equal to  $\Delta_x = \Delta_y = h$ , and  $h$  is determined so that a skin depth  $\delta$  of laser exceeds spatial mesh size  $h$ . In our simulation, we have  $h = 0.01\lambda$ . According to the mesh width  $h$ , a computational time interval is  $\tau = 0.005\lambda / c$ .

Plasma consists of protons or ions and electrons with a proton mass  $M = 1836m_e$ . Anywhere below the coordinates, time, density, momentum, and energy are given to be  $\lambda$ ,  $2\pi / \omega_0$ ,  $n_{\text{cr}}$ ,  $Mc$ ,  $Mc^2$ , respectively.

In the simulation, the foil density varies within  $25n_{\text{cr}} < n < 169n_{\text{cr}}$ , ( $n_{\text{cr}} = 1.1 \cdot 10^{21} \text{ cm}^{-3}$  for  $\lambda = 1 \text{ }\mu\text{m}$ ), the foil size  $d = 0.25\lambda$ . The amplitude

of a laser pulse has a range  $5 < a < 130$  ( $a = eE/m_e c \omega_0 = [I/(1.35 \cdot 10^{18} \text{ W/cm}^2) \cdot (\lambda/1 \mu\text{m})^2]^{1/2}$ ). The computational box has a uniform mesh with 100 cells per  $\lambda$ , and 200 particles per cell.

For the estimation accuracy of computer simulation we make a serial number of runs for a different numbers of particles in a cell  $N = 8, 32, 50, 200$ . The results of the test simulation show that a difference between the density amplitude for  $N = 50$  and  $N = 100$  is 2% and, for  $N = 200$  and  $N = 8$ , it is 10%. The main runs were carried out with 200 particles per cell. To solve the problem of the interaction of laser pulse with plasma it is necessary to consider several different temporal and spatial scales. As a result, a large number of calculations must be done, therefore the code UMKA2D3V was parallelized. The computer simulation was made on the computer complex SMP16X256 of the Siberian Supercomputer Center ICM&MG SB RAS.

### 3. Results of computer simulation

Let us consider the results of the computer simulation of the laser pulse-plasma interaction. The acceleration of ions in a thin foil by circular polarized laser pulse is based on the following physics. A laser pulse ionizes a foil and forms a slab of plasma, and pushes electrons forward by the radiation pressure. Ions are accelerated by a space-charge electric field created by separation of electrons and ions in plasma.

The contours of ion density  $n_i(x, y)$  for the initial parameters of the laser pulse and plasma  $a = 42$ ,  $n = 169$  are presented in Figure 1 at the times of 15 (a), 25 (b), and 55 (c) laser cycles from the beginning of the run. In the left frame, at  $t = 15$ , the initial stage of R-T instability is shown. One can see the evolution of the surface dynamics over several laser cycles.

A high density foil reflects the laser pulse almost totally and at the surface of overdense plasma a sharp density layer is formed ( $0 < t < 5$ ). Due to radiation pressure of a laser pulse plasma density significantly increases from  $n = 169$  ( $t = 0$ ) to  $n = 850$  ( $t = 10$ ) and then development of R-T

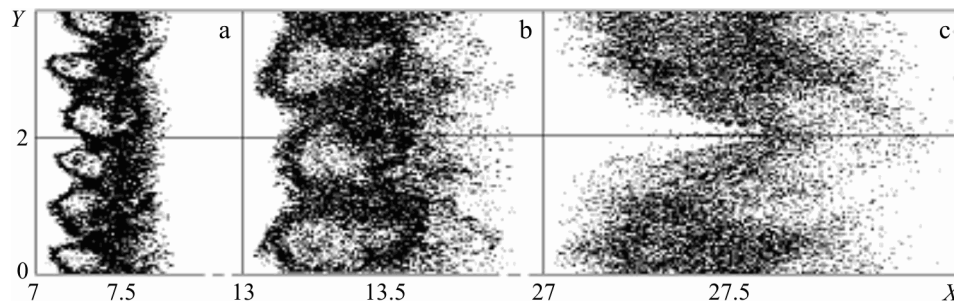


**Figure 1.** Contours of normalized ion density for  $a = 42$  and  $n = 169$  at various times in laser cycle units

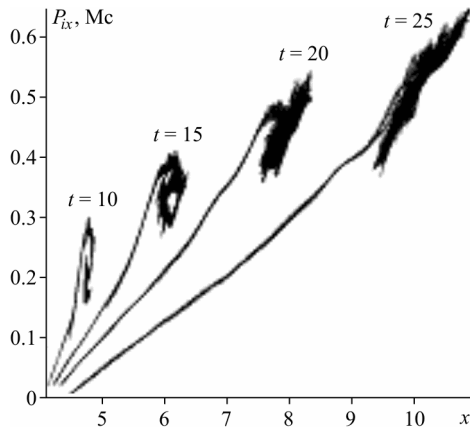


**Figure 2.** Ion phase space ( $P_{ix}, x$ ) for  $a = 32$  and  $n = 100$  at various times in laser cycle units

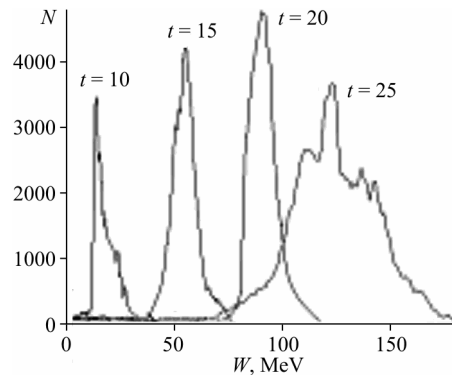


**Figure 3.** Ion energy spectrum for  $a = 32$  and  $n = 100$  at various times in laser cycle units

instability results in the deformation of foil and a stream formation. Initially, the foil has a uniform surface along  $y$ , and the change in its shape in time is due to the development of R-T instability. In the right frame at  $t = 55$ , we see the nonlinear stage of R-T instability with a low density of plasma. This instability develops with time over several laser periods. The growth of surface streams can be seen from Figure 1. At  $t = 15$ , they have a small wavelength  $L \approx 0.5\lambda$ , while, at  $t = 25$ , a wavelength  $L \approx 1\lambda$  and, at  $t = 55$ , the foil has a hole structure, i.e., the foil is destroyed. As a result, a laser pulse goes through plasma and the process of ion acceleration finishes.

The ion phase spaces ( $P_{ix}, x$ ) are presented in Figure 2. A significant amount of particles forms a definite loop giving a clear proof of the phase-stable acceleration driven by the laser radiation pressure. The ions trapped in a loop are accelerated to a mono-energy up to 100 MeV.

A foil can be fractured due to R-T instability, leading to the bunching of the foil and broadening of ion energy spectrum. The PIC model gives details of the ion energy distributions. The initial ( $t = 0$ ) ion distribution has the maxwellian shape. The ion energy spectrum at different moments presented in Figure 3. The energy spectrum is quasi-mono-energy beamlets for  $10 < t < 25$ . A fully nonlinear stage of instability results in the diffuse distribution for  $t > 25$ .

#### 4. Conclusion

To conclude, based on the 2D3V-PIC simulation, we have studied the problem of ion acceleration under interaction of super-intense circularly polarized laser pulse with overdense plasma target. The numerical simulation

shows a high rate of ion acceleration in RPA regime. The ponderomotive force of a circularly polarized laser pulse has no oscillations, and electrons can be steadily pushed forward. A charge separation field accelerates ions. The nonlinear development of R-T instability leads to the destruction of the foil and a decrease of ion acceleration rate. In this case, the laser pulse can penetrate into plasma, make holes, and ions cannot be steadily accelerated. Therefore, R-T instability of a plasma sheet is an obstacle to sustain a quasi-mono-energy regime of ion acceleration.

## References

- [1] Borghesi M., Fuchs J., Bulanov S.V., et al. Fast ion generation by high intensity laser irradiation of solid targets and application // *Fusion Sci. Technol.* — 2006. — Vol. 49, No. 412.
- [2] Mourou G., Tajima T., Bulanov S.V. Optics in the relativistic regime // *Review of Modern Physics.* — 2006. — Vol. 78. — P. 309–371.
- [3] Hegelich B.M., Albright B.J., Cobble J., et al. Laser acceleration of quasi-monoenergetic MeV ion beams // *Nature.* — 2006. — Vol. 4. — P. 439–441.
- [4] Liu C.S., Tripathi V.K., Shao X. Laser acceleration of monoenergetic protons trapped in moving double layer from thin foil // *Frontiers in Modern Plasma Physics: AIP Conference Proceedings.* — 2008. — Vol. 1061. — P. 246–254.
- [5] Ledingham K.W.D., Galster W., Sauerbrey R. Laser-driven proton oncology – a unique new cancer therapy // *Br. J. Radiol.* — 2007. — Vol. 80, No. 855.
- [6] Wilks S.C., Langdon A.B., Cowan T.E., et al. Energetic proton generation in ultra-intense laser-solid interactions // *Phys. Plasmas.* — 2001. — Vol. 8, No. 2. — P. 542.
- [7] Liseykina T.V., Bychenkov V.Yu., Dudnikova G.I., Pegoraro F. Laser-triggered ion acceleration at moderate intensity and pulse duration // *Applied Physics.* — 2005. — Vol. B, No. 81. — P. 537–542.
- [8] Maksimchuk A., Flippo K., Krauze Kh., et al. The generation of high energy ions by short laser pulses // *Plasma Physics.* — 2004. — Vol. 30, No. 6. — P. 473–496 (In Russian).
- [9] Pegoraro F., Bulanov S. Photon bubbles and ion acceleration in a plasma dominated by the radiation pressure of an electromagnetic pulse // *Phys. Rev. Lett.* — 2007. — Vol. 99.
- [10] Liseikina T., Prellino V., Cornolti F., Macchi A. Ponderomotive Acceleration of Ions: Circular Versus Linear Polarization. — *IEEE Trans Plasma Science*, 2008.
- [11] Badziak J., Jablonski S., Glowacz S. Generation of highly collimated high-current ion beams by skin-layer laser-plasma interaction at relativistic laserintensities // *Appl. Phys. Lett.* — 2006. — Vol. 89, — No 61504.

- [12] Eliasson B., Liu S.C., Shao Xi., et al. Laser acceleration of monoenergetic protons via a double layer emerging from an ultra-thin foil // *New Journal of Physics*. — 2009. — Vol. 11.
- [13] Pegoraro F., Bulanov S.V. Ion acceleration and stability in the radiation pressure dominated regime // *Laser Phys.* — 2009. — Vol. 19, No. 2. — P. 222–227.
- [14] Vshivkov V.A., Vshivkov K.V., Dudnikova G.I. Algorithms of solving the laser-plasma interaction problem // *J. Computational Technologies*. — 2001. — Vol. 6, No. 2.

